



# Poly-P-forming characteristics found in poly-P-accumulating microorganisms (phosphate-accumulating organisms [PAOs]) isolated from shrimp ponds in Vietnam

Tran Thi Huyen<sup>1,\*</sup>, Ha Phuong Trang<sup>1</sup>, Pham Thi Kim Phan<sup>1</sup>, Trinh Ngoc Nam<sup>2,\*</sup>

<sup>1</sup> Institute of Biotechnology and Food technology, Industrial University of Ho Chi Minh City, Ho Chi Minh City 72700, Vietnam

<sup>2</sup> Office of Science Management and International Affairs, Industrial University of Ho Chi Minh City, Ho Chi Minh City 72700, Vietnam

## Abstract

Significant amounts of phosphate ( $\text{PO}_4^{3-}$ ) in extensive shrimp ponds make an ideal survey for studying the  $\text{PO}_4^{3-}$ -accumulating properties of phosphate-accumulating organisms (PAOs) and harvesting polyphosphate (poly-P). In this study, we evaluated the  $\text{PO}_4^{3-}$ -accumulating capacities of four PAOs (A1, A2, A3, and A5) from those ponds by determining the residual  $\text{PO}_4^{3-}$ -content in acetate mineral mediums (AMM) with/without NaCl at different inoculated periods. Strain A2 was identified as a *Rhodotorula* sp., whereas strain A1 was *Acinetobacter guillouiae*, A3 was *Acinetobacter lwoffii*, and A5 was *Lactococcus raffinolactic*. Among four PAOs, strains A1 and A5 showed the highest  $\text{PO}_4^{3-}$ -accumulating capacities of 338.44 and 333.63  $\mu\text{g}$  in 100 mL of AMM, respectively, after 72 hours under cultural AMM without adding NaCl. All PAOs might extend the inoculation periods to 120 hours for mostly  $\text{PO}_4^{3-}$ -accumulations in the AMM with NaCl contents (5%–30‰) ( $p < 0.05$ ). The  $\text{PO}_4^{3-}$ -accumulation levels from 338.40 to 285.55  $\mu\text{g}$  of *Acinetobacter guillotine* demonstrated significantly higher capacities than the remaining PAOs ( $p < 0.05$ ), whereas the maximum  $\text{PO}_4^{3-}$ -collections of *L. raffinolactic* with 281.65  $\mu\text{g}/100$  mL recognized at single condition of NaCl content of 20‰, followed with 279.70  $\mu\text{g}/100$  mL by *A. lwoffii* at a NaCl content of 10‰. Upon the rate of  $\text{PO}_4^{3-}$ -accumulation correlated with growths in the LB medium with different salinities combined, the activities of the four PAOs did not alter the pH of the AMM, around 6.5 to 7.0, providing evidence for the impressing  $\text{PO}_4^{3-}$ -accumulating capacities of four PAO strains on different survival media conditions. This study is the first report on the accumulation of  $\text{PO}_4^{3-}$  to forming polyphosphate (poly-P) chains in *L. raffinolactic* cells; the other strains poly-P granules generated inside cells. Remarkably, our findings comprehensively discovered

Received: Jun 25, 2024 Revised: Aug 5, 2024 Accepted: Aug 25, 2024

\*Corresponding author: Tran Thi Huyen

Institute of Biotechnology and Food technology, Industrial University of Ho Chi Minh City, Ho Chi Minh City 71409, Vietnam

Tel: +84-2838940390, E-mail: [tranthihuyen@iuh.edu.vn](mailto:tranthihuyen@iuh.edu.vn)

\*Corresponding author: Trinh Ngoc Nam

Office of Science Management and International Affairs, Industrial University of Ho Chi Minh City, Ho Chi Minh City 72700, Vietnam

Tel: +84-2838940390, E-mail: [trinhngocnam@iuh.edu.vn](mailto:trinhngocnam@iuh.edu.vn)

This is an Open Access article distributed under the terms of the Creative Commons Attribution Non-Commercial License (<http://creativecommons.org/licenses/by-nc/4.0/>) which permits unrestricted non-commercial use, distribution, and reproduction in any medium, provided the original work is properly cited.

Copyright © 2024 The Korean Society of Fisheries and Aquatic Science

the forming process of poly-P in *A. guillotine* cells through image analysis at three inoculation times (0, 24, and 72 hours). These PAOs are viable probiotics that bring advantages in lowering abundant  $\text{PO}_4^{3-}$ -compounds in aquaculture wastewater and treating different  $\text{PO}_4^{3-}$ -polluted water resources. The poly-P in PAO cells promises valuable sources for harvesting poly-P applied in the fertilizer industry or biominerals.

**Keywords:** Acetate mineral medium (AMM), Diamidino-2-phenylindole dihydrochloride (DAPI), *Lactococcus raffinolactic*,  $\text{PO}_4^{3-}$ -accumulation capacities, poly-P accumulating microorganisms (phosphate-accumulating organisms [PAOs]), *Rhodotorula* sp.

## Introduction

In the seafood industry in Vietnam, shrimp accounts for approximately 40% of the total export turnover, bringing in nearly \$ 3.4 billion in 2022. Because of this sector's rapid growth and development, aquaculture wastewater in Vietnam is frequently dumped directly into natural water bodies, negatively affecting the aquaculture environment, biodiversity, and human habitats (Đôn, 2014). In addition, about 30% of nitrogen and 10% of phosphate ( $\text{PO}_4^{3-}$ ) from feed escape into the aquatic environment (Boyd, 2011). The abundant phosphate availability in a natural water environment is a typical reason for the dangerous eutrophication phenomenon (Yang et al., 2010). Therefore,  $\text{PO}_4^{3-}$ -removal in forming polyphosphate (poly-P) via microbial activities have recently increased interest because of its low costs, convenient operation, and environmental friendliness (Chu, 2006; Ngô, 2012). More specially, the application of poly-P as a reusable form for developing raw materials in the fertilizer industry or an alternative phosphate source in carp diet in recent approaches has triggered focus on phosphorus recovering solutions from many wastewater systems through the bacterial poly-P accumulation mechanisms (Hirota et al., 2010; Yoon et al., 2016). Thus, screening microbial strains that can accumulate phosphate  $\text{PO}_4^{3-}$  is not only an essential aspect of treating phosphorus compounds in the aquaculture wastewater system (Flowers et al., 2013; Oehmen et al., 2007), but also providing Poly-P for the fertilizer industry or biominerals from refined phosphate-accumulating organisms (PAOs) biomasses (Simoes et al., 2020; Yuan et al., 2012).

In water,  $\text{PO}_4^{3-}$  compounds are the simplest forms of accumulation poly-P into the microorganism cells. For example, the  $\text{PO}_4^{3-}$ -accumulating capacities of four PAOs, namely *Pseudomonas*, *Enterobacteriaceae*, *Alcaligenes*, and *Streptococcus* have recently been reported (Bao et al., 2007). However, their

$\text{PO}_4^{3-}$ -accumulating traits are still the subject of debate because *Acinetobacter* or *Accumulibacter phosphatis* shows  $\text{PO}_4^{3-}$ -accumulation but has never been cultured successfully in vitro experiments (Günther et al., 2009), in contrast to *Microlunatus phosphovorius* has even cultures in pure isolation but cannot determine precisely the  $\text{PO}_4^{3-}$ -accumulating capacities into the cells (Mao et al., 2015). Furthermore, applying  $\text{PO}_4^{3-}$  uptake assays can more conveniently confirm the  $\text{PO}_4^{3-}$ -accumulating capacity upon the remaining phosphate content in cultural media than other methods (Aravind et al., 2015; Chaudhry & Nautiyal, 2011). Therefore, evaluating the performance of  $\text{PO}_4^{3-}$ -removal systems is not always dependent on the proliferation of PAOs but also requires the successful in vitro cultivation of the PAOs (Tarayre et al., 2016).

Until now, intracellular poly-P of PAOs has also been detected as metachromatic granules, with an average size from 0.25 to 1.33  $\mu\text{M}$ , which are not visible unless stained. Each PAO strain can accumulate an average of 100 granules in its cell (Günther et al., 2009; Serafim et al., 2002). The most common technique used to verify the presence of intracellular poly-P is the poly-P granules stained with chemicals or fluorescent dyes before observing them under a light or fluorescence microscope (Serafim et al., 2002; Tarayre et al., 2016). Recently, 4',6-diamidino-2-phenylindole dihydrochloride (DAPI) dye with an optimal concentration of 10  $\mu\text{g}/\text{mL}$  of DAPI can confirm the presence of PAO in sludge samples through poly-P granules with a green-yellow fluorescence, whereas the DNA shows blue fluorescence (Günther et al., 2009; Klauth et al., 2006; Terashima et al., 2020). Besides, although electron microscopy is a powerful technique that allows the visualization of the cellular location of poly-P, this method cannot confirm the dynamics in the linkages of poly-P granules with other compartments inside the bacterial cell (Lima et al., 2003; Watanabe et al., 2021). Although the mechanisms of poly-P aggregation have been proposed (Gün-

ther et al., 2009; Hupfer et al., 2008; Simoes et al., 2020; Serafim et al., 2002; Terashima et al., 2020; Watanabe et al., 2021; Ye et al., 2015) however, the processes involved in the formation of the poly-P in the PAO cell are still largely unknown.

Following the argument mentioned above, the diverse exist of microbial strains that can accumulate  $\text{PO}_4^{3-}$  in an extensive shrimp pond in La Gi district, Binh Thuan Province in Vietnam at a nursing period of 4 to 5 months accrued significant amounts of phosphorus makes an ideal survey for studying the process and the accumulating properties of poly-P chains of PAOs. Our study successfully isolated four PAOs from eight colonies with a visibly resolved  $\text{PO}_4^{3-}$  zone on the selective acetate mineral mediums (AMM) agar plate from water and sludge samples of the shrimp pond. The  $\text{PO}_4^{3-}$ -accumulating capacities of four native PAOs (A1, A2, A3, and A5) and pH changes from the growth of PAOs in an AMM medium with and without five salt concentrations (from 0‰ to 30‰) at each differential cultural period were investigated detailedly. The high homologous identities of nucleotide sequences of the polymerase chain reaction (PCR) products with 16S rDNA deposited genes in GenBank determined strain A2 was a *Rhodotorula* sp. In contrast, strain A1 was *Acinetobacter guillouiae*, A3 was *Acinetobacter lwoffii*, and A5 was *Lactococcus raffinolactic*. Remarkably, fluctuations in the fluorescence properties between DNA and poly-P in the PAO cells during culturing comprehensively discovered the assembly of poly-P chains in *L. raffinolactic* (A5) and the generation of poly-P granules underlying  $\text{PO}_4^{3-}$ -accumulating in other strains, which can keep our knowledge about the poly-P accumulating process in PAO cells.

## Materials and Methods

### Isolation of phosphate-accumulating organisms (PAOs) and identification of their morphological properties

Isolating PAO strains were performed at an extensive shrimp pond with a pond area of 800–1,000 m<sup>2</sup> in La Gi district, Binh Thuan Province in Vietnam, after the breeding shrimp nursing period of 4 to 5 months. In October 2020, water and sludge samples from this pond were collected to screen PAOs. After collection, these samples were stored at 4°C–10°C and transported to the laboratory. One gram of the sludge sample and 50 mL of the water sample were placed into a beaker and gently mixed using a glass float to obtain a homogeneous representative sample. Subsequently, 1 mL of the representative sample was placed into a test tube containing 9 mL of 0.9% NaCl and mixed to obtain

the 10<sup>-1</sup> dilution. Five different ranges of bacterial suspensions from 10<sup>-2</sup> to 10<sup>-5</sup>, 50 µL of each diluted concentration, were plotted on plates containing selective AMM in triplicates and then incubated at a temperature of 25°C for 3–5 days in an incubator shaker at 30,000×g to isolate PAOs (Bao et al., 2007). After incubation, colonies forming clear surrounding halos were identified as PAOs (Nautiyal, 1999). Single colonies were sub-cultured on AMM to obtain pure colonies, which were examined microscopically and morphologically. Each colony differs in shape, color, and size, identified via Gram staining. Subsequently, potential PAOs were sub-cultured in a selective medium and spiked with 20% glycerol for storage at –70°C.

The antagonistic activity of PAOs was assessed by the streak line method on LB agar under aerobic conditions. First, 10 µL of each inoculated PAO strain (24 hours at 25°C) was streaked along a straight line on the LB agar plate with a transfer rod and dried. Next, the three remaining strains were streaked at right angles of the straight line before incubating the agar plate at 37°C for 24 or 48 hours. The antagonistic ability of all PAOs was determined by the inhibition zone (in millimeters) that appeared on the LB agar, ranked as high (> 25 mm), intermediate (13–25 mm), and low (0–12 mm) (Hütt et al., 2006; Nguyễn & Phan, 2014).

### Impact of the salt concentration on the growth of phosphate-accumulating organisms (PAOs) on LB medium

To determine the effect of the salt concentration on the growth of PAOs, the salt tolerance and thermal tolerance capacity of the isolates were checked by cultivating the strains in LB medium supplemented with NaCl at concentrations of 0‰, 5‰, 10‰, 20‰, and 30‰. Incubation time was 12 to 48 hours at 25°C. During the culture period, at surveying time points, 1 mL of the inoculated medium was aspirated and photometrically measured at 600 nm to investigate the impact of the salt concentration on growth was determined. All experiments were performed in triplicate.

### Accumulation of phosphate ( $\text{PO}_4^{3-}$ ) in acetate mineral mediums (AMM) and AMM supplemented with salt

#### *Phosphate ( $\text{PO}_4^{3-}$ ) accumulation in acetate mineral mediums (AMM)*

The  $\text{PO}_4^{3-}$ -solubilization is a crucial trait of bacteria and is routinely measured to assess  $\text{PO}_4^{3-}$ -accumulation of PAOs. Their growth in AMM was also investigated regarding the  $\text{PO}_4^{3-}$ -accumulation of PAOs. The composition of the AMM

medium was as follows (for 1 L): 10 g  $C_6H_{12}O_6$ , 5 g  $Ca_3(PO_4)_2$ , 5 g  $MgCl_2 \cdot 6H_2O$ , 0.25 g  $MgSO_4 \cdot 7H_2O$ , 0.2 g KCl, 0.1 g  $(NH_4)_2SO_4$ , 15 g agar. The  $PO_4^{3-}$ -accumulation was investigated by cultivating 500  $\mu$ L of isolated PAO stocks in test tubes containing 7 mL of AMM for 20 hours at 25 °C and 1.035 $\times$ g. After that, we transferred 1 mL of the culture medium to a conical flask containing 100 mL of AMM supplemented with 5%  $K_2HPO_4$ . The continuous culture's cultivation periods were 24, 48, 54, 72, 96, and 120 hours. For each period, the total volume was centrifuged at 7.168 $\times$ g for 10 min to collect the supernatant. Subsequently, 750 mM of Ames solution was sequentially added to 250  $\mu$ L of the supernatant, followed by incubation at 37 °C for 20 min for color development. The Ames solution consisted of 0.36% (w/v)  $(NH_4)_6Mo_7O_{24} \cdot 4H_2O$  in 1 N  $H_2SO_4$  plus 1.42% ascorbic acid and was prepared immediately before the assay. Each assay was performed in triplicate, and each isolate's average value was recorded as the  $PO_4^{3-}$ -accumulation capacity. Pure  $K_2HPO_4$  was used as the standard reagent. The  $PO_4^{3-}$ -accumulation capacity of PAOs was determined based on the residual  $PO_4^{3-}$ -content in the medium that reacted with ammonium molybdate to form a complex in an acidic environment. This complex is reduced sequentially by ascorbic acid to form a blue complex with an absorbance of 820 nm (Ames & Dubin, 1960; Barrows et al., 1985; Worsfold et al., 2005), which can be used to determine  $PO_4^{3-}$ -accumulation capacity of each PAO. The residual  $PO_4^{3-}$ -concentration in the medium was measured using a spectrophotometer (Genesys 10S UV-Vis, Thermo Scientific, Waltham, MA, USA) at 820 nm. The  $PO_4^{3-}$ -accumulation was calculated from the changes in absorbance, applying Equation (1):

$$R = (C_0 - C_t) \quad (1)$$

where  $C_0$  represents the initial concentration, and  $C_t$  indicates the concentration at time  $t$ .

#### **Measurement of phosphate accumulation in acetate mineral mediums (AMM) supplement with four salt concentrations**

As described above, 500  $\mu$ L of isolated PAO stocks in test tubes containing 7 mL of AMM at 25 °C with shaking at 1.035 $\times$ g for 24 to 48 hours, depending on each strain. After incubation, 1 mL of the culture was transferred to a conical flask containing 100 mL of AMM supplemented with 5%  $K_2HPO_4$  and NaCl at 5‰, 10‰, 20‰, and 30‰, followed by incubation at 25 °C under shaking at 1.035 $\times$ g. At different time points (24, 48, 72, 96, and 120 hours), samples were collected by centrifugation at

7.168 $\times$ g for 10 min to determine the concentration of  $PO_4^{3-}$  via spectrometry at 820 nm. The  $PO_4^{3-}$ -accumulation ability under different salt concentrations was calculated using Equation (1); each experiment was performed in triplicate.

#### **Molecular identification and phylogenetic analysis**

The genomic DNA of the four microbial strains was extracted using the 95 °C heat shock method. The extracted DNA was then used as template for PCR amplification with two pairs of primers specific for the 16S rDNA gene fragment. The forward primer was 27F (5'-GAGTTTGATCCTGGCTCAG-3'), and the reverse primer was 1492R (5'-AAGGAGGTGATCCAACC-3'). The primer for the ITS1 region of the forward sequence was ITS-F (5'-TCCGTAGGTGAACCTGCG-3'), and the reverse primer was ITS-R (5'-GCTGCGTTCTTCATCGATGC-3') (Bao et al., 2007; Mokhtari et al., 2011; Zhang et al., 2015). We used 5  $\mu$ L of template mixture for the PCR reaction. The PCR products were approximately 1.500 bp and 470 bp-long gene fragments of the 16S rDNA and ITS1 regions, respectively, and processed via 1.5% agarose electrophoresis. Subsequently, the harvested PCR amplicons were sequenced, and the final sequences were submitted to the GenBank database (National Center for Biotechnology Information, NCBI) to obtain the corresponding accession numbers.

The BLAST tool was used for phylogenetic analysis to search for homologous sequences previously published by other authors and stored in the NCBI. A phylogenetic tree was constructed using the MEGA 7.0 software, employing the neighbor-joining DNA distance algorithm with a bootstrap of 1.000. Then, comparing the position differences between species pairs using the software and building a phylogenetic tree based on the neighbor-joining method, the index at the base of the branches had a bootstrap value of 1.000 resampling times (%). The confidence level assessed according to the NJ bootstrap was below the high confidence level of > 85%; the average confidence level was 65%–85%, and the low confidence level was 65%, according to the MEGA 7.0 software.

#### **Microscopic observation of the accumulation of intracellular poly-P using diamidino-2-phenylindole dihydrochloride (DAPI) staining**

Firstly, ten  $\mu$ g/mL of DAPI (Sigma-Aldrich, St. Louis, MO, USA) (Tijssen et al., 1982) was used for staining 400  $\mu$ mol/g dry weight cell streaks containing poly-P and DNA particles. The accumulation of intracellular poly-P inside the cell was visualized by microscopic observation (Klauth et al., 2006; Streichan

et al., 1990). The bright yellow-fluorescent response of poly-P is a vital indicator for the discrimination of the blue-fluorescent DNA. First, 1 mL of the culture solution of the four PAO strains was grown proliferatively for five different culture periods and collected in a 1.5 mL Eppendorf tube, followed by centrifugation at  $3.200\times g$  for 5 min. The cell pellet was washed twice with 200  $\mu$ L of McIlvaine's buffer (two parts stock solution A:  $\text{BaCl}_2 \cdot 2\text{H}_2\text{O}$ , 5 mM  $\text{NiCl}_2 \cdot 6\text{H}_2\text{O}$  and eight parts stock solution B: 0.4 M  $\text{Na}_2\text{HPO}_4/\text{NaH}_2\text{PO}_4$ , 150 mM NaCl, pH 7.2) to remove any interfering substances (cellular debris or organic matter), resuspended in 4% formaldehyde, and incubated for 30 min at 25 °C. Next, the cell pellet was rewashed with 200  $\mu$ L of McIlvaine's buffer before being stained with DAPI. Subsequently, we dissolved 2 mg DAPI in 1 mL McIlvaine's buffer to prepare a stock solution with a concentration of 2 mg/mL and, subsequently, a working stock solution with a concentration of 10  $\mu$ g/mL for the following staining process (Serafim et al., 2002; Terashima et al., 2020; Watanabe et al., 2021). Next, to stain double-stranded DNA and poly-P with DAPI, 200  $\mu$ L of the working solution was added to the treated cell pellet, followed by incubation for an additional 30 min at room temperature (25 °C). The stained samples were centrifuged at  $1.080\times g$  for 5 min, and the pellets were resuspended in 20  $\mu$ L phosphate-buffered saline (PBS, pH 7.2, Sigma-Aldrich). Subsequently, 2  $\mu$ L of the stained mixture was subjected to fluorescence microscopy at the 450–650 nm range, with excitation at 360 nm (Serafim et al., 2002). The treatments were performed in triplicate.

### Other analyses and statistical analyses

Microbial growth and the pH values in the mixed liquid were monitored by an optical density (OD) analyzer and a pH analyzer, respectively. The OD concentration was determined by using a UV-Vis instrument at a wavelength of 600 nm. All statistical analyses were performed with GraphPad Prism 8.3.0. The data were subjected to a two-way analysis of variance (ANOVA). Specific differences between individual means from a set of standards were detected using Tukey's test, and differences at  $p < 0.05$  were considered significant.

## Results

### Selection and identification of the biological characteristics of phosphate-accumulating organisms (PAOs) on the acetate mineral mediums (AMM) medium

The 100  $\mu$ L of  $10^{-5}$  diluted solution samples from shrimp ponds

on sterilized AMM-selected isolated thirty-two colonies with various morphological characteristics, mainly milky white, milky white, yellow, or pink circular colonies. After that, eight colonies with a visible zone on the selective AMM agar plate were isolated as potential PAOs from the initially screened 32 strains with the ability to solubilize  $\text{PO}_4^{3-}$  (Supplementary Fig. 1S). Four of the colonies exhibited rates of  $\text{PO}_4^{3-}$ -solubilization over 50% in 48 hours and were selected as A1, A2, A3, and A5. The selected strains were then subjected to Gram staining to observe their morphological characteristics. As shown in Table 1, strains A1, A3, and A5 appeared as white colonies with a round shape and entire edges, whereas strain A2 had an oval shape and was pink. Strains A1, A3, and A5 were Gram-negative bacteria, whereas strain A2 was a yeast (Fig. 1). Subsequently, the strains were preserved in a freezer at  $-70^\circ\text{C}$  for the identification experiments.

### Effect of salt concentrations on the growth curves of the four selected phosphate-accumulating organism (PAO) strains in LB agar and their antagonistic properties

The absorbance of bacteria at 600 nm was used to estimate bacterial growth at the four NaCl concentrations. As shown in Fig. 2, the growth of A1, A2, and A3 did not differ significantly among the different salt concentrations ( $p > 0.05$ ), whereas strain A5 was affected considerably by NaCl, irrespective of the concentration. For A1, growth was most pronounced ( $\text{OD}_{600\text{nm}}$  of 1.3A), with negligible fluctuations. In contrast, the growth of strains A2, A3, and A5 changed slightly depending on the NaCl concentration. However, all strains showed decreased growth at a NaCl concentration of 30‰. At the highest salt concentration, strains A1 and A2 were more stable, with an  $\text{OD}_{600\text{nm}}$  around 1.1A, compared to the other strains, with a value of approximately 1.0A. The above differences may be explained by the different environments that interfered with the growth abilities of the strains. These results indicate that the different strains dif-

**Table 1. Morphological characteristics of four strains of PAOs**

Morphology characteristics	A1	A2	A3	A5
Colony shape	Circular	Oval	Circular	Circular
Surface	Wet	Wet	Wet	Rough
Edge	Entire	Entire	Erode	Entire
Color	White milk	Pink	White milk	White milk
Gram staining	Gram-negative		Gram-negative	Gram-negative

PAO, phosphate-accumulating organism.

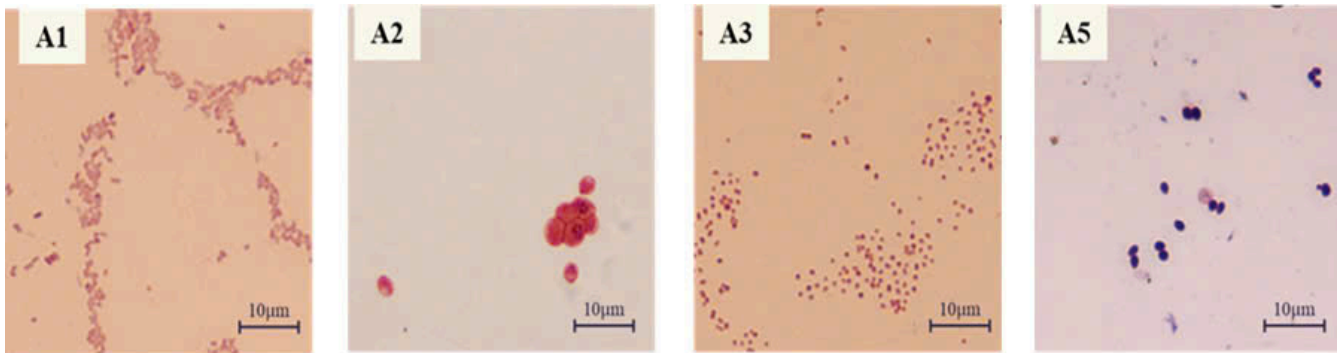


**Fig. 1. Morphological characteristics of the four PAO strains. Strains A1, A3, and A5 were Gram-negative bacteria, whereas strain A2 was yeast. PAO, phosphate-accumulating organisms.**

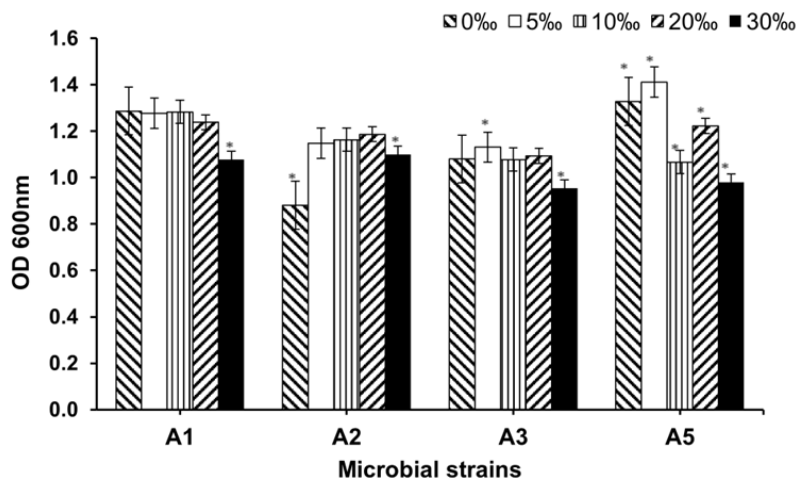


**Fig. 2. Effect of salt concentration on the growth of four PAOs (A1, A2, A3, and A5) on LB medium with adding NaCl concentration ranged to 0‰ to 30‰. Data represent mean ± SE (n = 3) statistical differences (\*p < 0.05) with Tukey's test.**

ferred in their ability to adapt to a salt concentration of 30‰.

**Molecular identification and phylogenetic tree construction**

According to previously described methods, the 16S rDNA gene sequencing was carried out for pure representative cultures of the four isolates. Hence, with the presence of PCR products of 1.500 bp for 16S rDNA primers and 470 bp for ITS1 primers on 1.5% agarose gel, each primer pair gave amplified products of the expected size (Fig. 3). These findings agreed with the results reported by Mokhtari et al. (2011). The amplified products were sequenced, and the 16S rDNA gene sequences of three strains, A1, A3, and A5, obtained 1.489 bp with stable signals. After submitting the 16S rDNA to the GenBank database and comparing it against known gene sequences using the BLAST

tool, the resulting sequences matched those of their respective type strains. Based on the aligned results, the DNA of strain A1 was 100% identical to that of *A. guillouiae* MT310710.1. The DNA of strain A3 showed 99.71% identity with that of *A. lwoffii* MH267196.1, and the DNA of strain A5 was 100% identical to that of *L. raffinolactic* HM058735.1. Finally, an aligned result of the ITS1 sequence region of the A2 strain of 450 bp stable nucleotides against known gene sequences using the BLASTn tool in NCBI showed a 100% similarity in nucleotide sequences with those of the genus *Rhodotorula* sp. MN268779.1.

The phylogenetic tree was built from the 16S rDNA sequences of strains A1, A3, and A5, compared to the NCBI. The diagram of the phylogenetic tree in Supplementary Fig. 2S shows that strains A1 and A3 belong to the genus in a subgroup

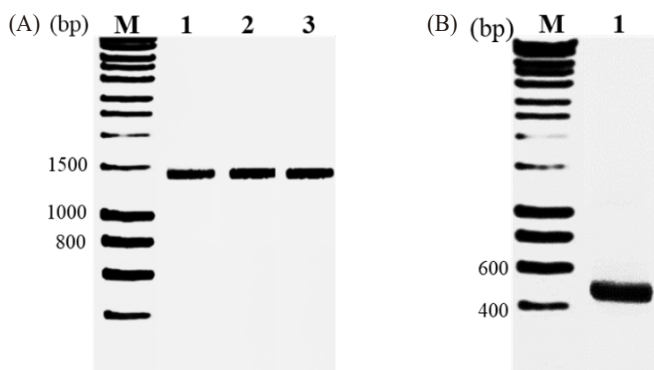


**Fig. 3. PCR results.** (A) PCR results of the 16S rDNA sequences of three strains A1, A3, and A5. Lane 1: Ladder DNA Bioline, Lane 2, 3, and 4: PCR results of 16S rDNA gene of the A1, A3, and A5 strains. (B) PCR results of the ITS1 region sequences of the A2 strain. PCR, polymerase chain reaction.

of the phylogenetic tree, with sequence similarity among species of the genus *Acinetobacter*, based on the NCBI database. Strain A1 showed no difference in base number compared with *A. guillotine* MT310710.1 with a bootstrap index of 100. Strain A3 differed from *A. lwoffii* MH267196.1 by a bootstrap index of 74. Unlike the above two strains, A5 was identified as *L. raffinolactic* HM058735.1 by a difference in the number of base sequences and a bootstrap index of 71 (Supplementary Fig. 3S). Similarly, the diagram in Supplementary Fig. 2S shows that strain A2 belongs to the genus *Rhodotorula* sp. MN268779.1, which has a base number difference in the sequence; the bootstrap index was 93.

Compared to the NCBI, the phylogenetic tree was built from the 16S rDNA sequences of strains A1, A3, and A5. The diagram of the phylogenetic tree in Supplementary Fig. 2S shows that strains A1 and A3 belong to the genus in a subgroup of the phylogenetic tree, with sequence similarity among species of the genus *Acinetobacter*, based on the NCBI database. Strain A1 showed no difference in base number compared with *A. guillotine* MT310710.1 with a bootstrap index of 100. Strain A3 differed from *A. lwoffii* MH267196.1 by a bootstrap index of 74. Unlike the above two strains, A5 was identified as *L. raffinolactic* HM058735.1 by a difference in the number of base sequences and a bootstrap index 71 (Supplementary Fig. 3S). Similarly, the diagram in Supplementary Fig. 2S shows that strain A2 belongs to the genus *Rhodotorula* sp. MN268779.1, which has a base number difference in the sequence; the bootstrap index was 93.

### Phosphate ( $\text{PO}_4^{3-}$ ) accumulation, growth behavior, and pH values of the four phosphate-accumulating organism (PAO) strains in acetate mineral mediums (AMM) with and without NaCl

#### Phosphate ( $\text{PO}_4^{3-}$ ) accumulation, growth behavior, and pH values in acetate mineral mediums (AMM)

After the inoculation periods, the residual  $\text{PO}_4^{3-}$ -content in the AMM was the  $\text{PO}_4^{3-}$ -accumulation from the  $\text{Ca}_3(\text{PO}_4)_2$  component of each PAO strain. Changes in cumulative values correlating to the  $\text{PO}_4^{3-}$ -accumulating ability of each PAO strain are shown in Fig. 4 and Table 2. Strains A1 and A5 showed gradually increasing  $\text{PO}_4^{3-}$ -accumulating capacities. In contrast, those of the remaining strains (A3 and A5) only described the fast acquisition in the initial 48 hours and the next time exhibited relatively constant, and finally did not involve any changes during later periods. The relative  $\text{PO}_4^{3-}$ -content in the AMM for each inoculation period, as shown in Table 2, revealed that strains A1 and A5 showed the highest respective accumulation, with 338.44 and 333.63  $\mu\text{g}/100\text{ mL}$  after 72 hours. In contrast, strain A3 only accumulated 256.42  $\mu\text{g}/100\text{ mL}$ . The lowest value was found for strain A2 with 130.19  $\mu\text{g}/100\text{ mL}$ . Because four PAOs lived and the  $\text{PO}_4^{3-}$ -content in the initial AMM solutions was not the same, it indicated the different accumulation capabilities of the PAOs ( $p < 0.05$ ).

The growth behavior and pH values in the selective AMM over 76 inoculation hours are shown in Fig. 4B. In general, the growth rate of the A3 strain was the lowest, and the difference in the growth of all four PAOs can be understood as a response to the different nutrient levels. Besides, the pH values measured during the inoculation periods fluctuated around 7.5 to 8. As seen in both Fig. 4A and 4B, although the  $\text{PO}_4^{3-}$ -accumulation efficiency of the A1 strain was not higher than that of the A5 strain, both showed the same growth behavior. Based on the initial  $\text{PO}_4^{3-}$ -accumulation in AMM, we further investigated the impact of salt concentration on  $\text{PO}_4^{3-}$ -collection of all PAOs.

#### Phosphate ( $\text{PO}_4^{3-}$ ) accumulation, growth behavior, and pH values in acetate mineral mediums (AMM) supplemented with five NaCl concentrations

Fig. 5 shows the  $\text{PO}_4^{3-}$ -accumulation of the four PAO strains in AMM medium with a  $\text{PO}_4^{3-}$ -content of 340  $\mu\text{g}/100\text{ mL}$  supplemented with NaCl at five different concentrations (5‰, 10‰, 20‰, and 50‰). The fluctuations in the remaining  $\text{PO}_4^{3-}$ -content showed a slight impact of the NaCl concentration on  $\text{PO}_4^{3-}$ -accumulation for all four PAOs ( $p < 0.05$ ). As shown

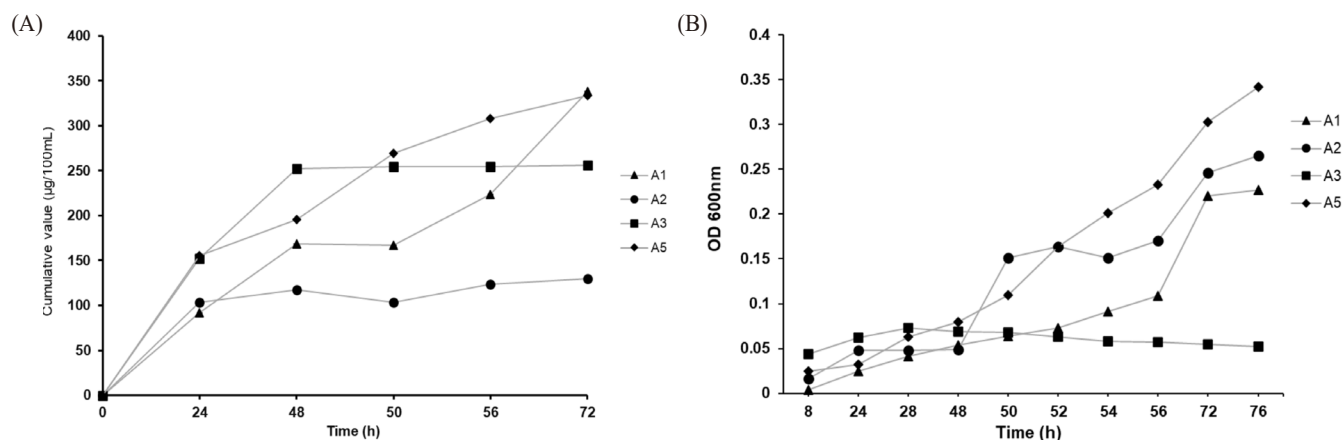


**Fig. 4. The PO<sub>4</sub><sup>3-</sup>-accumulation and biomass growth of four PAOs in AMM medium.** (A) The PO<sub>4</sub><sup>3-</sup>-accumulation of four PAOs (A1, A2, A3, and A5) in AMM medium; (B) Biomass growth measured by optical density 600 nm of four PAOs (PAOs [*Acinetobacter guillouiae* - A1; *Rhodotorula* sp - A2; *Acinetobacter lwoffii* - A3; and *Lactococcus raffinolactic* - A5]) in AMM medium. Data represent mean ± SE (n = 3) statistical differences (p < 0.05) with Tukey's test. PO<sub>4</sub><sup>3-</sup>, phosphate; PAO, phosphate-accumulating organism.

in Table 2, strain A1 led the best performance, with efficiencies of 338.40 and 321.29 µg/100 mL at salt concentrations of 5‰–10‰ and a lower cumulative efficiency of 285.55 µg/100 mL at salt concentrations of 20‰–30‰ after 120 hours of culturing (p < 0.05). We observed independent variations in PO<sub>4</sub><sup>3-</sup>-accumulation for A3 and A5; the maximum collection was found for A5, with 281.65 µg/100 mL at a NaCl content of 20‰, followed by that for A3 with 279.70 µg/100 mL at a NaCl content of 10‰. Except for the A2 strain, adding NaCl content from 5‰–30‰ enhanced its PO<sub>4</sub><sup>3-</sup>-accumulation, resulting in an accumulation efficiency of 246.80–277.92 µg/100 mL after 120 hours of cultivation. Without NaCl addition, the maximum accumulation efficiency was 130.19 µg/100 mL after 72 hours of cultivation. These findings show that the microbial strains isolated here have been treated with the PO<sub>4</sub><sup>3-</sup>-content in an AMM medium with different salt concentrations.

**Characteristics of PO<sub>4</sub><sup>3-</sup> migration and poly-P accumulation**

Because intracellular poly-P cannot easily be observed without staining (Serafim et al., 2002), digital image analysis allowed us to visualize poly-P in PAO cells after 72 hours of cultivation in AMM under aerobic conditions (Mino et al., 1998). In a 2 µL sample containing each PAO stained with ten µg/mL DAPI, the type of poly-P forms inside the PAO cells could be distinguished by yellow-green fluorescence emission in contrast to the blue fluorescence of DNA (Fig. 6). After 72 hours of incubation, the yellow fluorescence of strains A1 and A5 was more intense than

that of strains A2 and A3. DNA surrounded Poly-P in the cells of three PAO strains (A1, A3, and A5). In strains A1 and A3, poly-P comprised concentrated granules with yellow-green fluorescence, whereas A5 consisted of a poly-P chain. The location and contributions of poly-P and DNA particles in each PAO sample were observed in bright-field images. The fluorescence signals of poly-P for strains A1 and A3 were like those reported for *Corynebacterium glutamicum* (Klauth et al., 2006).

Fig. 7 shows the distribution of the yellow fluorescence signal of poly-P compared to that of the DNA for all PAOs at 0, 48, and 72 hours of incubation. The amount of poly-P fluorescence in all four PAOs substantially increased after 24 hours, followed by a rising population of poly-P in a sequential period to obtain the high intensity of the poly-P at 72 hours. Analysis of the poly-P content dynamics allowed us to determine the characteristics of the four PAOs. Remarkably, upon the profiles of the contribution of the yellow fluorescence contents in the *A. guillotine* cells (A1) strain, we can propose a PO<sub>4</sub><sup>3-</sup>-accumulation process beginning by slight yellow fluorescence responding to PO<sub>4</sub><sup>3-</sup>-content at the 0h inoculation time, followed by conjunction of yellow-green fluorescence of granule poly-P was linked to yellow-green fluorescence of DNA at 24 hours. At the end time of 72 hours, a phenomenon of concentrated poly-P granules with yellow fluorescence surrounded by DNA range was observed clearly inside *A. guillotine* cells (A1).

**Table 2. Possibility of PO<sub>4</sub><sup>3-</sup>-accumulation of PAOs and four reference strains including *Streptococcus*, *Alcaligenes*, *Pseudomonas*, *Enterobacteriaceae***

Strains	Salt content (%)	Cumulative value (µg/100 mL) at survey time intervals (h)						pH after 120 h
		0	24	48	72	96	120	
<i>Acinetobacter guillouinae</i> (A1)	0	0.00 <sup>a</sup> ± 0.00	91.94 <sup>b</sup> ± 0.014	168.58 <sup>c</sup> ± 0.011	338.44 <sup>d</sup> ± 0.002	ND	ND	7–8.5
	5	0.00 <sup>a,2</sup> ± 0.00	31.93 <sup>a,3</sup> ± 0.067	152.26 <sup>b,4</sup> ± 0.011	243.78 <sup>c,5</sup> ± 0.941	301.16 <sup>d,6</sup> ± 0.03	338.40 <sup>e,7</sup> ± 0.003	
	10	0.00 <sup>a,2</sup> ± 0.00	60.39 <sup>a,b</sup> ± 0.097	130.63 <sup>b,3</sup> ± 0.027	224.10 <sup>a,4</sup> ± 0.095	299.10 <sup>b,5</sup> ± 0.01	321.29 <sup>b,6</sup> ± 0.002	
	20	0.00 <sup>a,2</sup> ± 0.00	34.85 <sup>a,3</sup> ± 0.014	107.75 <sup>b,4</sup> ± 0.079	207.16 <sup>c,5</sup> ± 0.080	285.73 <sup>d,6</sup> ± 0.01	285.55 <sup>e,7</sup> ± 0.019	
	30	0.00 <sup>a,2</sup> ± 0.00	34.85 <sup>a,3</sup> ± 0.014	116.62 <sup>b,4</sup> ± 0.035	207.18 <sup>c,5</sup> ± 0.080	285.73 <sup>d,6</sup> ± 0.01	285.56 <sup>e,7</sup> ± 0.019	
<i>Rhodotorula</i> sp. (A2)	0	0.00 <sup>a</sup> ± 0.00	103.28 <sup>b</sup> ± 0.011	117.16 <sup>b</sup> ± 0.034	130.19 <sup>b</sup> ± 0.046	ND	ND	7–9
	5	0.00 <sup>a,2</sup> ± 0.00	87.08 <sup>b,3</sup> ± 0.043	80.70 <sup>b,4</sup> ± 0.052	134.80 <sup>b,5</sup> ± 0.080	250.52 <sup>d,6</sup> ± 0.04	275.71 <sup>d,7</sup> ± 0.067	
	10	0.00 <sup>a,2</sup> ± 0.00	15.96 <sup>a,3</sup> ± 0.032	66.33 <sup>b,4</sup> ± 0.019	132.66 <sup>c,5</sup> ± 0.046	214.78 <sup>d,6</sup> ± 0.05	277.92 <sup>e,7</sup> ± 0.059	
	20	0.00 <sup>a,2</sup> ± 0.00	26.78 <sup>a,3</sup> ± 0.068	31.48 <sup>a,b</sup> ± 0.019	188.80 <sup>b,5</sup> ± 0.034	241.57 <sup>c,6</sup> ± 0.06	242.81 <sup>c,7</sup> ± 0.072	
	30	0.00 <sup>a,2</sup> ± 0.00	24.74 <sup>a,3</sup> ± 0.024	49.04 <sup>b,4</sup> ± 0.037	154.13 <sup>c,5</sup> ± 0.071	223.65 <sup>d,6</sup> ± 0.00	244.58 <sup>d,7</sup> ± 0.042	
<i>Acinetobacter lwoffii</i> (A3)	0	0.00 <sup>a</sup> ± 0.00	152.58 <sup>b</sup> ± 0.051	252.59 <sup>b</sup> ± 0.002	256.42 <sup>b</sup> ± 0.003	ND	ND	7–8
	5	0.00 <sup>a,2</sup> ± 0.00	119.54 <sup>b,3</sup> ± 0.11	197.23 <sup>c,4</sup> ± 0.027	206.80 <sup>c,5</sup> ± 0.076	232.90 <sup>d,6</sup> ± 0.07	246.80 <sup>d,7</sup> ± 0.080	
	10	0.00 <sup>a,2</sup> ± 0.00	118.65 <sup>b,3</sup> ± 0.03	184.63 <sup>c,4</sup> ± 0.015	233.00 <sup>d,5</sup> ± 0.066	263.74 <sup>e,6</sup> ± 0.06	279.70 <sup>f,7</sup> ± 0.057	
	20	0.00 <sup>a,2</sup> ± 0.00	130.90 <sup>b,3</sup> ± 0.07	149.70 <sup>c,4</sup> ± 0.11	174.00 <sup>d,5</sup> ± 0.037	198.28 <sup>d,6</sup> ± 0.04	255.31 <sup>e,7</sup> ± 0.041	
	30	0.00 <sup>a,2</sup> ± 0.00	24.74 <sup>a,b</sup> ± 0.12	49.04 <sup>a,c</sup> ± 0.049	154.13 <sup>b,5</sup> ± 0.045	223.65 <sup>c,6</sup> ± 0.06	244.58 <sup>c,7</sup> ± 0.081	
<i>Lactococcus raffinolactis</i> (A5)	0	0.00 <sup>a</sup> ± 0.00	155.41 <sup>b</sup> ± 0.040	195.36 <sup>c</sup> ± 0.017	333.63 <sup>d</sup> ± 0.017	ND	ND	7–8.5
	5	0.00 <sup>a,2</sup> ± 0.00	34.58 <sup>b,3</sup> ± 0.069	81.15 <sup>c,4</sup> ± 0.030	110.23 <sup>c,5</sup> ± 0.015	146.77 <sup>d,6</sup> ± 0.02	186.77 <sup>e,7</sup> ± 0.022	
	10	0.00 <sup>a,2</sup> ± 0.00	43.63 <sup>b,3</sup> ± 0.027	68.11 <sup>c,4</sup> ± 0.026	70.86 <sup>c,5</sup> ± 0.037	150.50 <sup>d,6</sup> ± 0.00	207.15 <sup>e,7</sup> ± 0.076	
	20	0.00 <sup>a,2</sup> ± 0.00	56.05 <sup>b,3</sup> ± 0.115	55.34 <sup>b,4</sup> ± 0.027	101.81 <sup>c,5</sup> ± 0.085	153.42 <sup>d,6</sup> ± 0.02	281.65 <sup>e,7</sup> ± 0.058	
	30	0.00 <sup>a,2</sup> ± 0.00	41.50 <sup>b,3</sup> ± 0.04	75.83 <sup>c,4</sup> ± 0.020	121.32 <sup>d,5</sup> ± 0.034	135.86 <sup>d,6</sup> ± 0.03	213.23 <sup>e,7</sup> ± 0.06	
<i>Streptococcus</i>	ND	174	ND	ND	ND	ND	ND	ND
<i>Alcaligenes</i>	ND	224	ND	ND	ND	ND	ND	ND
<i>Pseudomonas</i>	ND	1,434	ND	ND	ND	ND	ND	ND
<i>Enterobacteriaceae</i>	ND	91	ND	ND	ND	ND	ND	ND

All data has presented as mean ± SE (n = 3) statistical differences (p < 0.05) with Multiple's ranges test. The initial values provided differences of each inoculate period. The second value provided differences of each NaCl content. Data from Bao et al. (2007).

PO<sub>4</sub><sup>3-</sup>, phosphate; PAO, phosphate-accumulating organism; ND, not detected.

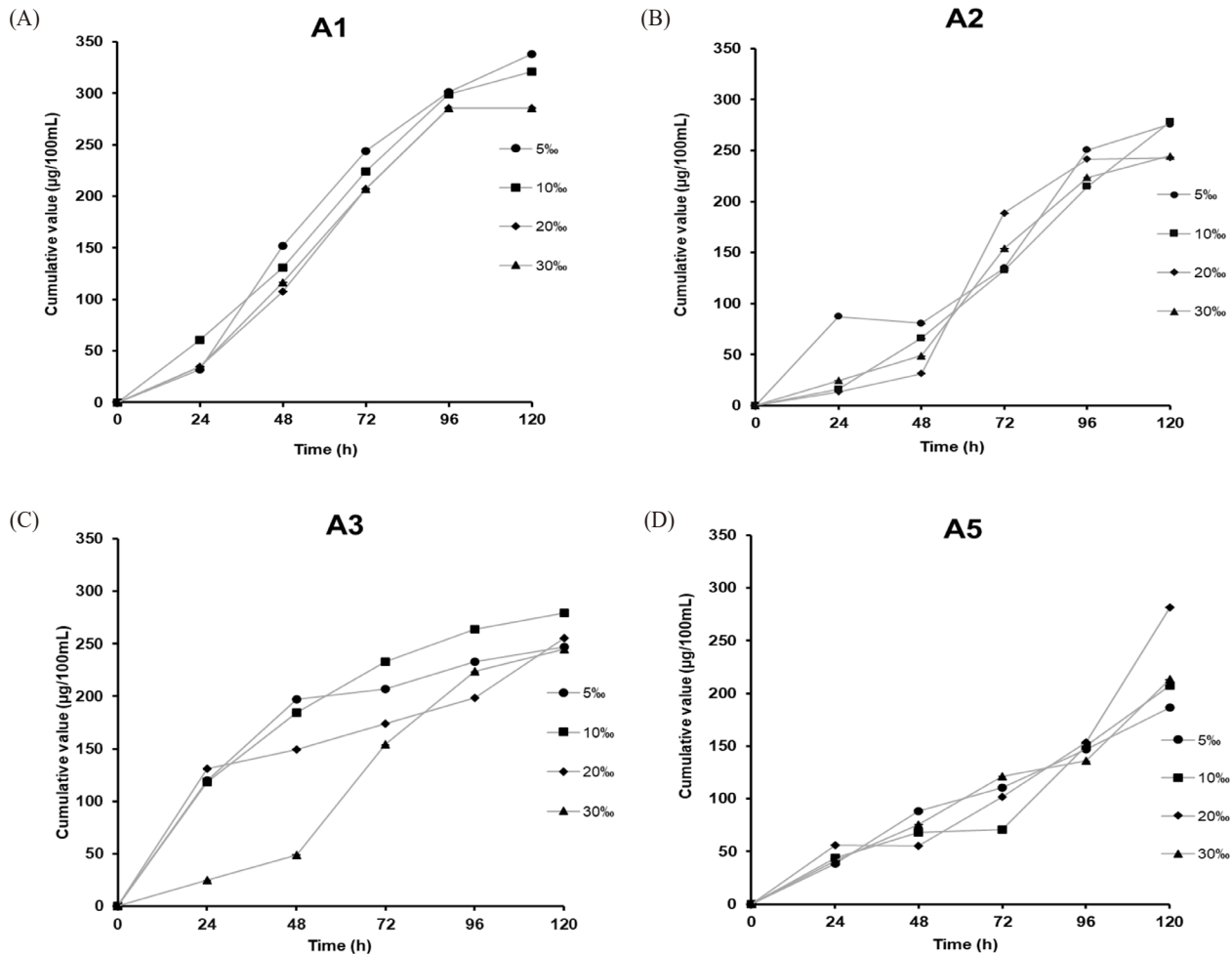


**Fig. 5. The  $PO_4^{3-}$ -accumulation of four PAOs (A1, A2, A3, and A5) in AMM selective medium supplemented with salt.** Data represent mean  $\pm$  SE (n = 3) statistical differences ( $p < 0.05$ ) with Tukey's test.  $PO_4^{3-}$ , phosphate; AMM, acetate mineral mediums.

## Discussion

PAOs, integral microorganisms in the natural phosphorus cycle, have recently attracted interest due to their effective  $PO_4^{3-}$ -accumulation activity from aqueous solutions (Stokholm-Bjerregaard et al., 2017). This study successfully applied a commonly suitable approach to isolating PAOs involved in  $PO_4^{3-}$ -accumulation ability by cultivating microorganisms in AMM. Their scientific names identified all four PAOs through phylogenetic analysis of conserved gene sequences performed for bacterial 16S rDNA and yeast ITS1 region. Among these, three bacteria, A1, A3, and A5, were found, including *A. guillotine*, *A. lwoffii*, and *L. raffinolactic*, while the fourth, A2, was identified as

*Rhodotorula* sp.

With the lowest residual  $PO_4^{3-}$ -content in the AMM with or without NaCl demonstrated, only *A. guillotine* got the highest  $PO_4^{3-}$ -accumulation efficiencies during most inoculated periods compared to the three remaining strains. Next, adding NaCl content in the AMM revealed different trends in  $PO_4^{3-}$ -accumulating capacities of all PAOs ( $p < 0.05$ ). Although all PAOs might extend the inoculation periods to 120 hours for almost  $PO_4^{3-}$ -accumulations in the NaCl-added AMM, *A. guillotine* showed a declined gradual impact of the  $PO_4^{3-}$ -accumulation in AMM with ascending NaCl content (5% to 30%), whereas the maximum  $PO_4^{3-}$ -collections of *L. raffinolactic* with 281.65 µg/100 mL recognized at single condition of NaCl content of

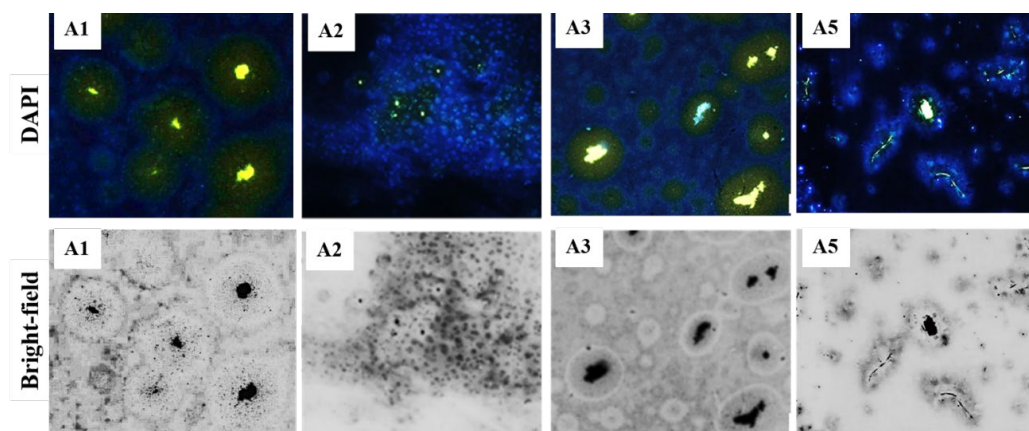


**Fig. 6. DAPI staining of DNA and poly-P maintaining intracellular viability after inoculating 72 hours in an AMM selective medium of four PAOs (*Acinetobacter guillouiae* - A1; *Rhodotorula* sp - A2; *Acinetobacter lwoffii* - A3; and *Lactococcus raffinolactic* - A5) began from left to right.** The images above are fluorescence images using the DAPI staining, and the images below are the bright-field image. The presence of DNAs emitted blue fluoresces, and poly-P emitted yellow green fluoresces. DAPI, 4',6-diamidino-2-phenylindole dihydrochloride; poly-P, polyphosphate; AMM, acetate mineral mediums; PAO, phosphate-accumulating organism.

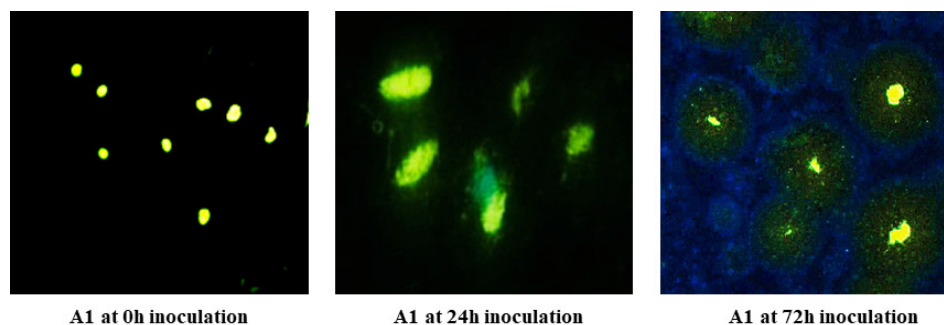


**Fig. 7. DAPI staining of DNA and poly-P of the *Acinetobacter guillouiae* strain presented intracellular viability from 24 to 72 hours during inoculation.** The images above show that DNA fluorescents are blue, and poly-P fluorescents are yellow green. DAPI, 4',6-diamidino-2-phenylindole dihydrochloride; poly-P, polyphosphate.

20‰, followed that value was 279.70  $\mu\text{g}/100\text{ mL}$  by *A. lwoffii* at a NaCl content of 10‰. One important thing is that only single yeast, such as *Rhodotorula* sp., first determined in this study, not only shows a higher capacity to accumulate  $\text{PO}_4^{3-}$  in the AMM than that in *A. lwoffii* but also can more effectively accumulate the  $\text{PO}_4^{3-}$ -content in the AMM containing NaCl at 5‰–30‰.

A comparative analysis of  $\text{PO}_4^{3-}$ -accumulation efficiencies between four PAOS and four reference strains, Enterobacteriaceae, Streptococcus, Alcaligenes, and Pseudomonas, were summarized and displayed in Table 2. Except for Pseudomonas with the highest  $\text{PO}_4^{3-}$ -accumulating efficiency (1.434  $\mu\text{g}$ ), three strains (Enterobacteriaceae, Streptococcus, Alcaligenes) with

accumulation levels of 91, 174, and 224  $\mu\text{g}$  (Bao et al., 2007) show the  $\text{PO}_4^{3-}$ -accumulating efficiencies were lower than three PAO strains (*A. guillouiae*, *Rhodotorula* sp., and *L. raffinolactic*). Furthermore, the  $\text{PO}_4^{3-}$ -accumulating capacities with different salinities combined maintain the pH of the AMM, around 6.5 to 7.0, providing evidence for the excellent adaptability of all four PAOs on survival conditions containing NaCl at 5‰–30‰. These results indicated impressing  $\text{PO}_4^{3-}$ -accumulation behaviors of four PAOs compared to other referenced strains.

Poly-P has been constituted by an aggregation of  $\text{PO}_4^{3-}$ , with an astounding number of activities performed in the cell. However, the most recent reports have yet to explain the

$\text{PO}_4^{3-}$ -accumulating process of PAO in depth (Long et al., 2021). Previous studies reported poly-P content uptake in PAO cells during a batch cultural period from the large to the stationary phase with almost no fluctuations (Klauth et al., 2006; Zheng et al., 2020). On the other hand, although cytosolic poly-P presents a green fluorescence throughout the *C. glutamicum* cell (Klauth et al., 2006), this observation has not yet been displayed dynamically in connection to other components in the cell (Serafim et al., 2002). In addition, most studies on the observation of stored poly-P inside microorganisms, such as *M. phosphovorus*, *Pseudomonas* spp., and *Paracoccus* spp., detected and quantified in the granule conformations (Günther et al., 2009; Klauth et al., 2006; Terashima et al., 2020). Therefore, results from the present study proposed the first evidence of the assembly of poly-P chains in *L. raffinolactic* (A5) against the generation of poly-P granules in the three remaining strains. Remarkably, our findings comprehensively discovered the forming process of poly-P from fluctuations in the fluorescence signals of DNA and poly-P in *A. guillotine* cells through image analysis at three inoculation times (0, 24, and 72 hours); these results deepened our knowledge about the poly-P accumulating process in PAO cells.

Finally, although in explanation of the results comparing the distinct  $\text{PO}_4^{3-}$ -accumulation abilities of four PAO strains in vitro investigation summarized here, the study has its limitations, such as cultural conditions and small scale that have yet to be fully simulated in natural environments. Hence, we proposed further research directions, such as testing the ability of PAO strain to treat wastewater on a larger scale and consequently in natural environments. In addition, studying the effects of other environmental factors (such as temperature and pH) on the process of poly-P accumulation is also available evidence to gain knowledge of the different properties of poly-P accumulation in each PAO strain.

## Conclusion

The present research defined the  $\text{PO}_4^{3-}$ -accumulation abilities from the 5 g  $\text{Ca}_3(\text{PO}_4)_2$  component in the AMM and the poly-P acquisition efficiency into PAO cells during 72 inoculate hours. These  $\text{PO}_4^{3-}$ -accumulative processes have proven that all PAOs accumulated  $\text{PO}_4^{3-}$  in the AMM into poly-P in the PAO cells. The best  $\text{PO}_4^{3-}$ -accumulative efficiencies were *A. guillotine* (A1) and *L. raffinolactic* (A5), with 338.44 and 333.63  $\mu\text{g}$  in 100 mL of AMM, respectively, after 72 hours under cultural AMM

without adding NaCl. Notably, *Rhodotorula* sp. showed higher  $\text{PO}_4^{3-}$ -accumulating capacities in higher NaCl-containing AMMs from 5%–30%. Although the NaCl contents (5%–30%) slightly impacted inoculation time for the  $\text{PO}_4^{3-}$ -accumulating capacities of PAOs, the activities of the four PAOs did not alter the pH of the AMM, around 6.5 to 7.0, providing evidence for the impressive  $\text{PO}_4^{3-}$ -accumulating capacities of four PAO strains on different survival media conditions. With poly-P stained with DAPI, this study is the first report on the accumulation of  $\text{PO}_4^{3-}$  to forming poly-P chains in *L. raffinolactic* cells against poly-P granules generated in cells of other strains. Based on distribution changes of poly-P at three inoculation periods (0, 24, and 72 hours), we can see the forming process of poly-P in *A. guillotine* cells. The  $\text{PO}_4^{3-}$  removal in forming poly-P via microbial activities of four PAOs in this study are compelling features to support sustainable solutions for treating different  $\text{PO}_4^{3-}$ -polluted water resources and further promises to provide valuable sources for harvesting -contained compounds that are applied in the fertilizer industry or biominerals from biomasses.

## Supplementary Materials

Supplementary materials are only available online from: <https://doi.org/10.47853/FAS.2024.e71>

### Competing interests

No potential conflict of interest relevant to this article was reported.

### Funding sources

Not applicable.

### Acknowledgements

Tran Thi Huyen conceived and designed the experiments, performed the experiments, analyzed the data, prepared figures and/or tables, authored or reviewed drafts of the paper and approved the final draft. Ha PhuongTrang, Pham Thi Kim Phan performed the experiments, prepared figures and/or tables. Trinh Ngoc Nam, Tran Thi Huyen critically reviewed the manuscript and approved the final draft. All authors read and approved the final manuscript.

### Availability of data and materials

Upon reasonable request, the datasets of this study can be available from the corresponding author.



- sis] Hanoi: Đại Học Quốc Gia Hà Nội; 2012.
- Nguyễn VP, Phan TPT. Phân lập, định danh và xác định các đặc tính có lợi của chủng *Bacillus* spp. từ ao nuôi tôm ở tỉnh Bến Tre. Tạp chí Khoa học. 2014;64:94.
- Oehmen A, Lemos PC, Carvalho G, Yuan Z, Keller J, Blackall LL, et al. Advances in enhanced biological phosphorus removal: from micro to macro scale. Water Res. 2007;41:2271-300.
- Serafim LS, Lemos PC, Levantesi C, Tandoi V, Santos H, Reis MAM. Methods for detection and visualization of intracellular polymers stored by polyphosphate-accumulating microorganisms. J Microbiol Methods. 2002;51:1-18.
- Simoes F, Colston R, Rosa-Fernandes C, Vale P, Stephenson T, Soares A. Predicting the potential of sludge dewatering liquors to recover nutrients as struvite biominerals. Environ Sci Ecotechnol. 2020;3:100052.
- Stokholm-Bjerregaard M, McIlroy SJ, Nierychlo M, Karst SM, Albertsen M, Nielsen PH. A critical assessment of the microorganisms proposed to be important to enhanced biological phosphorus removal in full-scale wastewater treatment systems. Front Microbiol. 2017;8:718.
- Streichan M, Golecki JR, Schön G. Polyphosphate-accumulating bacteria from sewage plants with different processes for biological phosphorus removal. FEMS Microbiol Ecol. 1990;6:113-24.
- Tarayre C, Nguyen HT, Brognaux A, Delepierre A, de Clercq L, Charlier R, et al. Characterisation of phosphate accumulating organisms and techniques for polyphosphate detection: a review. Sensors. 2016;16:797.
- Terashima M, Kamagata Y, Kato S. Rapid enrichment and isolation of polyphosphate-accumulating organisms through 4',6-diamidino-2-phenylindole (DAPI) staining with fluorescence-activated cell sorting (FACS). Front Microbiol. 2020;11:793.
- Tijssen JPF, Beekes HW, Van Steveninck J. Localization of polyphosphates in *Saccharomyces fragilis*, as revealed by 4',6-diamidino-2-phenylindole fluorescence. Biochim Biophys Acta Mol Cell Res. 1982;721:394-8.
- Watanabe T, Kitamura Y, Aizawa H, Masuki H, Tsujino T, Sato A, et al. Fluorometric quantification of human platelet polyphosphate using 4',6-diamidino-2-phenylindole dihydrochloride: applications in the Japanese population. Int J Mol Sci. 2021;22:7257.
- Worsfold PJ, Gimbert LJ, Mankasingh U, Omaka ON, Hanrahan G, Gardolinski PCFC, et al. Sampling, sample treatment and quality assurance issues for the determination of phosphorus species in natural waters and soils. Talanta. 2005;66:273-93.
- Yang YG, He ZL, Lin Y, Stoffella PJ. Phosphorus availability in sediments from a tidal river receiving runoff water from agricultural fields. Agric Water Manag. 2010;97:1722-30.
- Ye Y, Gan J, Hu B. Screening of phosphorus-accumulating fungi and their potential for phosphorus removal from waste streams. Appl Biochem Biotechnol. 2015;177:1127-36.
- Yoon TH, Won S, Lee DH, Choi JW, Ra C, Kim JD. Effect of a new phosphorus source, magnesium hydrogen phosphate (MHP) on growth, utilization of phosphorus, and physiological responses in carp *Cyprinus carpio*. Fish Aquat Sci. 2016;19:39.
- Yuan Z, Pratt S, Batstone DJ. Phosphorus recovery from wastewater through microbial processes. Curr Opin Biotechnol. 2012;23:878-83.
- Zhang H, Huang T, Chen S. Ignored sediment fungal populations in water supply reservoirs are revealed by quantitative PCR and 454 pyrosequencing. BMC Microbiol. 2015;15:44.
- Zheng L, Wu X, Ding A, Wang S, Zhang S, Xie E. Phosphorus release and uptake of a denitrifying phosphorus-accumulating bacterium with different electron acceptors. Appl Ecol Environ Res. 2020;18:7865-80.